

N92-14350

THE STABILITY OF THE STEADY STATE AND BISTABLE RESPONSE OF A  
FLEXIBLE ROTOR SUPPORTED ON SQUEEZE FILM DAMPERS\*

Meng Guang  
The Vibration Research Council  
Northwestern Polytechnical University  
Xian, China

In this paper, the stability of the steady state circular response and the bistable response of a flexible rotor--centralised squeeze film damper (shortened as SFD) system is analysed, and the system's characteristics of accelerating or decelerating through the bistable region are investigated. It is found that there are two unstable regions for the circular response. The larger the unbalance parameter and the smaller the bearing parameter and external damping, the easier it is to cause an unstable circular response. In addition, the larger mass ratio and the smaller stiffness ratio will decrease the threshold rotating speed of instability. Although in some cases, the system's circular response is unstable, the system is still stable and has stable nonsynchronous response.

It is also found that only when the initial rotating speed is ahead of the bistable region can the bistable response be produced when the system is accelerating through the bistable region. The small solution of the bistable response is more stable than the large one.

NOMENCLATURE

a	= angle acceleration
B	= bearing parameter ( $=\mu RL^3/m_B \omega_c^3$ ), where R is the bearing radius, L is land length of SFD, and $\mu$ is the absolute viscosity of the lubricant
c	= radial clearance of SFD
$c_d$	= external damping coefficient
$e_u$	= unbalance eccentricity
$k_a$	= retainer spring stiffness
$k_s$	= shaft stiffness
K	= stiffness ratio ( $=k_a/k_s$ )
$m_B, m_D$	= mass lumped at bearing station and rotor mid-span
$m_u$	= unbalance mass for experiment
n	= rotating speed in RPM
U	= unbalance parameter ( $=e_u/c$ )

\*Supported by the Aviation Scientific Foundation of China.

$x, y; r, t$  = Cartesian and polar coordinates  
 $X, Y$  =  $x/c, y/c$   
 $\bar{Z}$  =  $X+iY$   
 $\bar{Z}$  = conjugation of  $Z$   
 $\alpha$  = mass ratio ( $=m_B/m_D$ )  
 $\epsilon_B, \epsilon_D$  = eccentricity ratio of journal or disk ( $=e_B/c$  or  $e_D/c$ ), where  
 $e_B$  and  $e_D$  are eccentricities  
 $\beta$  = damping ratio ( $=c_d/2m_D\omega_c$ )  
 $\Gamma$  =  $a/\omega_c^2$   
 $\phi_B, \phi_D$  = attitude angles  
 $\omega$  = rotor rotating speed  
 $\omega_c$  = pin-pin critical speed ( $=(k_s/m_D)^{1/2}$ )  
 $\Omega$  = speed ratio ( $=\omega/\omega_c$ )  
 $\tau$  =  $\omega t$  for steady state response and  $\omega_c t$  for transient response  
 $(\cdot)$  =  $d/dt$   
 $(')$  =  $d/d\tau$

### Subscripts

$(B)$  = bearing journal  
 $(D)$  = disk  
 $(o)$  = steady state condition  
 $(x), (y)$  = direction subscripts

## INTRODUCTION

A well designed squeeze film damper (SFD) is a good isolator and damper in rotating machinery and can increase the system's stability. But poorly designed SFD may destabilize the rotor system, so the stability analyses of rotors supported on SFD's have received more attention (Ref. 1 and Ref. 2). The bistable response which is induced by the nonlinear fluid film forces will cause a large vibration amplitude that is harmful to the rotor system. Since the high nonlinearity of the fluid film force makes the mathematical analysis very difficult, most stability analyses of the rotor-SFD system are limited to the case of steady state circular response of the centralised SFD system (Ref. 3 and Ref. 4). Whether the system is unstable when its circular response is unstable is still an undiscussed problem. As the system is nonlinear, it may have a stable response other than the circular response. Furthermore, it is not clear what the properties are when the rotor system accelerates through the bistable region, and the influences of the system parameters on the system's stability have not been thoroughly analysed. As these problems are very important for designing good SFD, they are worth investigating.

## EIGEN-MATRIX FOR STABILITY ANALYSIS

For the flexible rotor supported on the centralised SFD shown in Fig. 1, the nondimensional equations of motion can be derived by taking the same assumptions adopted in Ref. 5:

Bearing journal:

$$z''_B + \frac{1}{2\alpha\Omega^2} [(1+K) z_B - z_D] = \frac{2B}{\Omega} F \quad (1)$$

$$z''_D + \frac{2\beta}{\Omega} z'_D + \frac{1}{\Omega^2} (z_D - z_B) = U e^{i\tau} \quad (2)$$

where  $F = f_x + i f_y$  is the dimensionless fluid film force.

In the assumptions of the short bearing and  $\pi$ -film, there are (ref. 6)

$$\begin{cases} f_x = -\frac{1}{(X_B^2 + Y_B^2)^{1/2}} [X_B(\epsilon_B \phi'_B I_1 + \epsilon'_B I_2) - Y_B(\epsilon_B \phi'_B I_3 + \epsilon'_B I_1)] \\ f_y = -\frac{1}{(X_B^2 + Y_B^2)^{1/2}} [Y_B(\epsilon_B \phi'_B I_1 + \epsilon'_B I_2) + X_B(\epsilon_B \phi'_B I_3 + \epsilon'_B I_1)] \end{cases} \quad (3)$$

where

$$I_1 = \int_{\theta_1}^{\theta_1 + \pi} \frac{\sin \theta \cos \theta}{(1 + \epsilon_B \cos \theta)^3} d\theta, \quad I_2 = \int_{\theta_1}^{\theta_1 + \pi} \frac{\cos^2 \theta}{(1 + \epsilon_B \cos \theta)^3} d\theta, \quad I_3 = \int_{\theta_1}^{\theta_1 + \pi} \frac{\sin^2 \theta}{(1 + \epsilon_B \cos \theta)^3} d\theta$$

$$\theta_1 = \arctan[-\epsilon'_B / (\epsilon_B \phi'_B)], \quad \epsilon_B = (X_B^2 + Y_B^2)^{1/2}, \quad \phi_B = \arctan(Y_B / X_B)$$

For the steady state circular response, there are

$$z_{B0} = \epsilon_0 e^{i\phi_0}, \quad \epsilon_0 = \text{const}, \quad \phi_0 = \tau - \phi_1, \quad \phi_1 = \text{const} \quad \text{and} \quad z_{B0} = i z_{B0}$$

Linearizing the nonlinear fluid film force about the steady state circular response  $z_{B0}$  with the Taylor series, we get (Ref. 6)

$$F = F_0 + A_1 z_2 + (B_1 + iC_1) e^{2i\phi_0} \bar{z}_2 + A_2 z'_2 + (B_2 + iC_2) e^{2i\phi_0} \bar{z}'_2, \quad (4)$$

where,  $z_2 = z_B - z_{B0}$ . The linearizing coefficients are

$$\begin{cases} F_0 = (K_0 + iC_0) z_{B0} \\ A_1 = \frac{(3 + \epsilon_0^2) \epsilon_0}{(1 - \epsilon_0^2)^3}, \quad B_1 = \frac{(5\epsilon_0^2 - 1) \epsilon_0}{(1 - \epsilon_0^2)^3}, \quad C_1 = \frac{3\pi \epsilon_0^2}{2(1 - \epsilon_0^2)^{5/2}} \\ A_2 = \frac{\pi(2 + \epsilon_0^2)}{4(1 - \epsilon_0^2)^{5/2}}, \quad B_2 = \frac{3\pi \epsilon_0^2}{4(1 - \epsilon_0^2)^{5/2}}, \quad C_2 = \frac{2\epsilon_0^2}{2(1 - \epsilon_0^2)^2} \end{cases} \quad (5)$$

and

$$K_0 = \frac{2\epsilon_0}{(1-\epsilon_0^2)^2} \quad , \quad C_0 = \frac{\pi}{2(1-\epsilon_0^2)^{3/2}}$$

As  $\epsilon_0 = \text{const}$ ,  $\phi_0 = \tau - \phi_1$ ,  $\phi_1 = \text{const}$ , it can be seen that these coefficients are periodic functions of time, the period being  $\pi$ .

In Eq. (1) and Eq. (2), note  $Z_1 = Z_D - Z_{DO}$ ,  $Z_2 = Z_B - Z_{BO}$ , we can get the perturbed equations of motion about the steady state response

$Z_{BO} = \epsilon_0 e^{i\phi_0}$  and  $Z_{DO} = \epsilon_{DO} e^{i\phi_{DO}}$  (approximated to the first order term):

$$\begin{cases} Z_1'' + \frac{2\beta}{\Omega} Z_1' + \frac{1}{\Omega^2} (Z_1 - Z_2) = 0 \\ Z_2'' + \frac{1}{2\alpha\Omega^2} [(1+K)Z_2 - Z_1] = -\frac{2B}{\Omega} [A_1 Z_2 + (B_1 + iC_1) e^{2i\phi_0} \bar{Z}_2 + A_2 Z_2' \\ \quad + (B_2 + iC_2) e^{2i\phi_0} \bar{Z}_2'] = 0 \end{cases} \quad (6)$$

Thus, the perturbed equations of motion of the system about its circular response are in the form of the Hill equation with periodic coefficients.

Now  $U_1 = p_1 + i p_2$ ,  $U_2 = p_3 + i p_4$ , and make the transformation of

$$Z_1 = U_1 e^{i\phi_0}, \quad Z_2 = U_2 e^{i\phi_0} \quad (7)$$

that is, analysing the problem in the coordinate rotating synchronously with the rotor shaft, we have

$$Z_1 = U_1 e^{i\phi_0}, \quad Z_1' = (U_1' + iU_1) e^{i\phi_0}, \quad Z_1'' = (U_1'' + 2iU_1' - U_1) e^{i\phi_0} \quad (8)$$

There are similar results for  $Z_2$ . Substituting Eq. (7) and Eq. (8) into Eq. (6) and separating the real and imaginary parts, we get

$$P'' + DP' + SP = 0 \quad (9)$$

where  $P = (p_1, p_2, p_3, p_4)^T$ , and the damping matrix  $D$  and stiffness matrix  $S$  are

$$D = \begin{bmatrix} \frac{2\beta}{\Omega} & -2 & 0 & 0 \\ 2 & \frac{2\beta}{\Omega} & 0 & 0 \\ 0 & 0 & \frac{2B}{\Omega}(A_2+B_2) & \frac{2B}{\Omega}C_2-2 \\ 0 & 0 & \frac{2B}{\Omega}C_2+2 & \frac{2B}{\Omega}(A_2-B_2) \end{bmatrix}$$

$$S = \begin{bmatrix} \frac{1}{\Omega^2}-1 & -\frac{2\beta}{\Omega} & 0 & 0 \\ \frac{2\beta}{\Omega} & \frac{1}{\Omega^2}-1 & 0 & 0 \\ -\frac{1}{2\alpha\Omega} & 0 & \frac{1+K}{2\alpha\Omega^2}-1+\frac{2B}{\Omega}(A_1+B_1+C_2) & -\frac{2B}{\Omega}(A_2+B_2-C_1) \\ 0 & -\frac{1}{2\alpha\Omega} & \frac{2B}{\Omega}(A_2-B_2+C_1) & \frac{1+K}{2\alpha\Omega^2}-1+\frac{2B}{\Omega}(A_1-B_1-C_2) \end{bmatrix}$$

Substituting Eq. (5) into Eq. (9) and noting  $R = (r_1, r_2, \dots, r_8)^T$   
 $= (p_1, p_1', p_2, p_2', p_3, p_3', p_4, p_4')^T$ , Eq. (9) can be transferred to the first order form:

$$\frac{dR}{d\tau} = HR \quad (10)$$

Note

$$C_{rr} = \frac{\pi(1+2\epsilon_o^2)}{2(1-\epsilon_o^2)^{5/2}}, \quad C_r = \frac{2\epsilon_o}{(1-\epsilon_o^2)^2}, \quad C_{sr} = \frac{2\epsilon_o}{(1-\epsilon_o^2)^2}, \quad C_{ss} = \frac{\pi}{2(1-\epsilon_o^2)^{3/2}}$$

$$K_{rr} = \frac{4\epsilon_o(1+\epsilon_o^2)}{(1-\epsilon_o^2)^3}, \quad K_{rs} = -\frac{\pi}{2(1-\epsilon_o^2)^{3/2}}, \quad K_{sr} = \frac{\pi(1+2\epsilon_o^2)}{2(1-\epsilon_o^2)^{5/2}}, \quad K_{ss} = \frac{2\epsilon_o}{(1-\epsilon_o^2)^2}$$

These are the same eight fluid film force coefficients commonly used for SFD in the polar coordinate (Ref. 4); then the coefficients matrix  $H$  is

$$H = \begin{bmatrix}
 0 & 1 & 0 & 0 & 0 & 0 & 0 & 0 \\
 1 - \frac{1}{\Omega^2} & -\frac{2\beta}{\Omega} & \frac{2\beta}{\Omega} & 2 & \frac{1}{\Omega^2} & 0 & 0 & 0 \\
 0 & 0 & 0 & 1 & 0 & 0 & 0 & 0 \\
 -\frac{2\beta}{\Omega} & -2 & 1 - \frac{1}{\Omega^2} & -\frac{2\beta}{\Omega} & 0 & 0 & \frac{1}{\Omega} & 0 \\
 0 & 0 & 0 & 0 & 0 & 1 & 0 & 0 \\
 \frac{1}{2\alpha\Omega^2} & 0 & 0 & 0 & 1 - \frac{1+K}{2\alpha\Omega^2} - \frac{2B_K}{\Omega} r_{rr} & -\frac{2B_C}{\Omega} r_{rr} & -\frac{2B_K}{\Omega} r_{rs} & 2 - \frac{2B_C}{\Omega} r_{rs} \\
 0 & 0 & 0 & 0 & 0 & 0 & 0 & 1 \\
 0 & 0 & \frac{1}{2\alpha\Omega^2} & 0 & -\frac{2B_K}{\Omega} s_{sr} & -2 - \frac{2B_C}{\Omega} s_{sr} & 1 - \frac{1+K}{2\alpha\Omega^2} - \frac{2B_K}{\Omega} s_{ss} & -\frac{2B_C}{\Omega} s_{ss}
 \end{bmatrix} \quad (11)$$

The stability of the system's steady state circular response can be determined by the eigenvalue of matrix  $H$ . The steady state responses  $Z_{BO}$  and  $Z_{DO}$  of Eq. (1) and Eq. (2) are asymptotically stable when all the eigenvalues of  $H$  have negative real parts, and they are unstable if only one eigenvalue of  $H$  has a positive real part.

#### NUMERICAL ANALYSIS OF STABILITY

The eigenvalues of matrix  $H$  are solved with the QR method, and the stability of the system's steady state circular response is analysed. From numerical results we find that, for both  $\Omega < 1$  and  $\Omega > 1$ , there are two unstable regions. The unstable region generally begins before the peak point of response and finishes after the peak point (see Fig. 2). In most cases, the larger the unbalance parameter  $U$ , and the smaller the bearing parameter  $B$  and the external damping ratio  $\beta$ , the easier it is to produce the unstable response. Furthermore, the larger the mass ratio  $\alpha$  and the smaller the stiffness ratio  $K$ , the lower the threshold rotating speed of instability - perhaps because the larger  $\alpha$  and smaller  $K$  may reduce the critical speed of the system. No instability is found in the region of  $\Omega < 1$  and  $\varepsilon_0 < 0.5$ .

The middle solution of the bistable response is always unstable, while the small solution is always stable. For the bistable response of the isolated bifurcation form, the large solution is generally stable (see Fig. 3), but it may be unstable when the bistable region is large (see Fig. 4). For the bistable response of the Duffing form

when  $\Omega < 1$  (although in most cases the large solution is stable) it may become unstable in some cases (see Fig. 2). When  $\Omega > 1$ , the large solution is unstable in most cases (see Fig. 2 and Fig. 3).

In order to find the reason for this instability, Eq. (1) and Eq. (2) are directly solved with the Runge-Kutta method in the unstable region. It is found that in most cases, the instability is caused by the nonsynchronous response. That is to say, within the unstable region, although the circular response is unstable, the system is still stable and has a stable, nonsynchronous response. For the example of Fig. 3, when  $\Omega = 2.0$ , the circular response is unstable, but the system has a stable  $1/3$  subharmonic response at the same time (see Fig. 5).

Besides the nonsynchronous response, the lack of a steady state response is another reason for instability. In only a few cases, the system is very unstable, and the response is divergent.

The above results explain the reason why the bistable response is seldom found in practical rotor systems, although it is common in theoretical analyses.

From the numerical results it is also found that the instability can be avoided by selecting reasonable system parameters, especially for the instability in  $\Omega < 1$ .

It is worth paying special attention to the fact that the nonsynchronous response also occurs frequently in centralised SFD, both in the regions of  $\Omega < 1$  and  $\Omega > 1$  although the nonsynchronous response may be more prevalent in the uncentralised SFD. The nonsynchronous response should be avoided as it will cause alternating fatigue to the rotor system.

#### TRANSIENT CHARACTERISTICS WHEN THIS SYSTEM IS ACCELERATING THROUGH THE BISTABLE REGION AND STABLE DEGREE OF BISTABLE RESPONSE

We have analysed the stability of bistable response. But what is the bistable jumping process, and what is its relationship with the initial rotating speed? Furthermore, the large and small solutions of the bistable response are both stable in most cases, but which is more stable? So the transient response of the system accelerating through a bistable region is analysed in the following.

Supposing that the accelerating motion of the flexible rotor---centralised SFD system has a constant acceleration, that is,  $\phi'' = \text{const} = a$ , then the dimensionless equations of motion can be written as

$$\left\{ \begin{array}{l} Z_D'' + 2\beta Z_D' + Z_D - Z_B = U\phi^2 e^{i\phi} - iU\Gamma e^{i\phi} \\ Z_B'' + \frac{1}{2\alpha} [(1+K)Z_B - Z_D] = 2BF \\ \phi'' = \Gamma, \quad \phi' = \Gamma\tau + \Omega_0, \quad \phi = \Gamma\tau^2/2 + \Omega_0\tau + \phi_0 \end{array} \right. \quad (12)$$

where  $\tau$  is now denoted as  $\tau = \omega_C t$  and  $\Omega_0$  is the initial speed ratio.

By solving Eq. (12) numerically, we find that, for different initial rotating speeds at the beginning of acceleration, the response routes when passing through the bistable region are different. If we note the beginning and finishing speed ratio of the Duffing bistable

response as  $\Omega_s$  and  $\Omega_e$  (see Fig. 6), then the response will take the route of L1 when  $\Omega_0 < \Omega_s$ , and a bistable response occurs (see Fig. 7). But the response after jumping down will not completely take the route of the steady state response, it goes to steady state after a period of oscillation. During the period of oscillation, a nonsynchronous response appears in some cases. When the initial speed ratio  $\Omega_0 > \Omega_s$ , only for very suitable initial response conditions can the response take the large solution and cause bistable jumping. In most cases, the response will take the route of L2; that is, the small solution is the practical one and no bistable jumping occurs. If  $\Omega_0 < \Omega_s$ , but stops accelerating when  $\Omega_s < \phi\Omega_e$ , then the bistable jumping down will occur in most cases, and when the acceleration is continued, the response will take the route of L2. Therefore, the response will take the route of L3 for the whole process.

From the above analysis, it can be seen that the small solution of the bistable response is more stable than the large one. In decelerating, the response takes the route of L4. It is easy to see that the jumping phenomenon of deceleration is not obvious and sudden as that of acceleration, and the faster the deceleration, the smaller the jumping amplitude.

## EXPERIMENTAL ANALYSIS

In this experiment, a symmetric rotor is used which has a diameter of 32 mm and a length of 889 mm, with a 10.325 kg disk assembled in its mid-span. The SFD is fabricated with two load lands, a circumferential groove for the oil supply, and no seals. The first rigid critical speed of the rotor shaft is about 5500 RPM, the absolute viscosity of the lubricant at 18 °C is about  $\mu = 8.05 \times 10^{-8}$  kgs/cm.

The rotor and journal vibrations in the horizontal and vertical directions are measured and recorded by a TEAC-R50C type recorder and then processed with an SM-2100B signal analyser. This gives us the magnitudes of vibration, the oscillation orbits, and the power spectrum charts of the response.

Figure 8 is the stable nonsynchronous response of 1/2 the sub-harmonic. Although theoretical analyses show that, in this case, the steady state circular response of the system is unstable, the system is still stable.

Figure 9 shows a stable synchronous (almost circular) response and theoretical analyses also indicate that the circular response is stable.

Figure 10 shows the experimental results of a bistable jumping down when system is accelerating through the bistable region. It can be seen that the middle solution of the bistable response is unstable, as shown in the orbit figure.

## CONCLUSIONS

1. The perturbed equations of motion of a flexible rotor supported on SFD about its circular response are of the form of Hill equations with periodic coefficients, and there are two unstable regions for the system's circular response separately in  $\Omega < 1$  and  $\Omega > 1$ . In most cases,

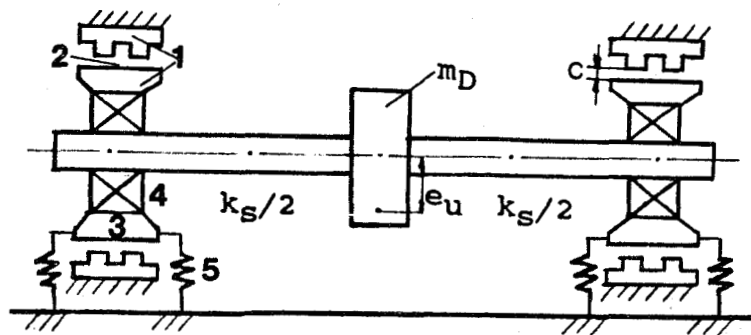
the larger the unbalance parameter and the smaller the bearing parameter and external damping, the easier it is to produce instability. Furthermore, larger mass ratio and small stiffness ratio will decrease the threshold rotating speed of instability.

2. Although the steady state circular response is unstable, the system is still stable in most cases and has a stable nonsynchronous response. In many cases, especially when  $\Omega > 1$ , the large solution of bistable response is also unstable, and then bistable jumping will not occur. This explains why the bistable response is seldom observed in practical rotor systems. Thus further work on bistable response is not worth pursuing.

3. Whether the bistable jumping occurs or not is largely related to the initial rotating speed where acceleration begins. Only when the initial speed is ahead of the bistable region can the bistable jumping be caused. The small solution of the bistable response is more stable than the large one.

#### REFERENCES

- [1] Tonneson, J.; Lund, J.W., "Some Experiments on Instability of Rotor Supported in Fluid Film Bearing," Trans. of ASME. J. of Mechanical Design, Vol. 100, No. 1, 1978, pp. 147-155.
- [2] Yan Litang, "The Bistable Characteristics of Rigid Rotor Supported on Squeeze Film Dampers," Proc. of Fourth Conf. on Structure, Strength and Vibration, 1987, China, pp. 76-78.
- [3] Rabinowitz, M.D.; Hahn, E.J., "Stability of Squeeze Film Damper Supported Flexible Rotors," ASME paper 77-GT-51.
- [4] White, D.C., "The Dynamics of a Rigid Rotor Supported on Squeeze Film Bearings," Proc. Inst. mech. Engrs. Vol. 186, 1972, pp. 213-219, Conf. on Vibration in Rotating System.
- [5] Meng Guang; Xue Zhonggong, "Investigation on Steady State Response and its Nonlinear Characteristics of Flexible Rotor--Squeeze Film Damper System," ASME paper 85-DET-141.
- [6] Meng Guang; Xue Zhonggong, "Some Theoretical Analyses on Flexible Rotor--Squeeze Film Damper Bearings System and Fluid Film Forces," Proc. of the Intl. Conf. on Rotordynamics, Sept. 1986, Tokyo, pp. 511-516.



1. squeeze film damper
2. squeeze oil film
3. outer race constrained not to rotate
4. ball bearing
5. centralising spring

Fig.1 Schematic diagram of a flexible rotor with squeeze film damper

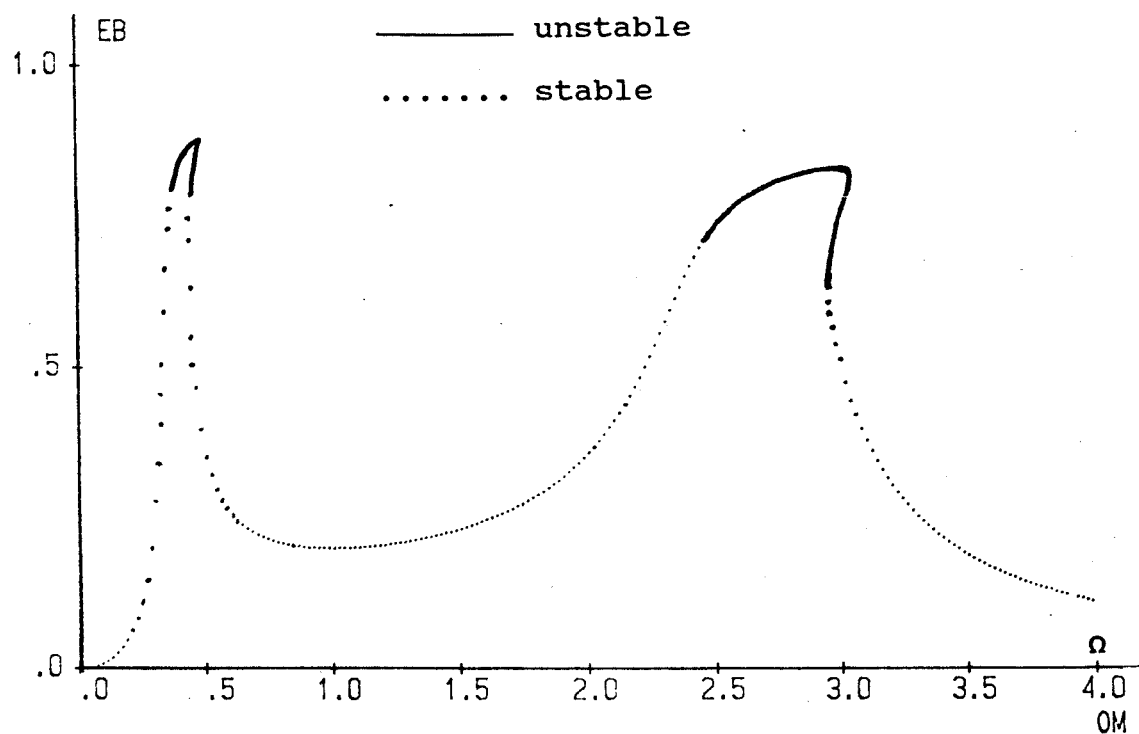


Fig.2 Stability analysis of system's circular response  
 $(U=0.2, \beta=0.0005, \alpha=0.1, B=0.025, K=0.2)$

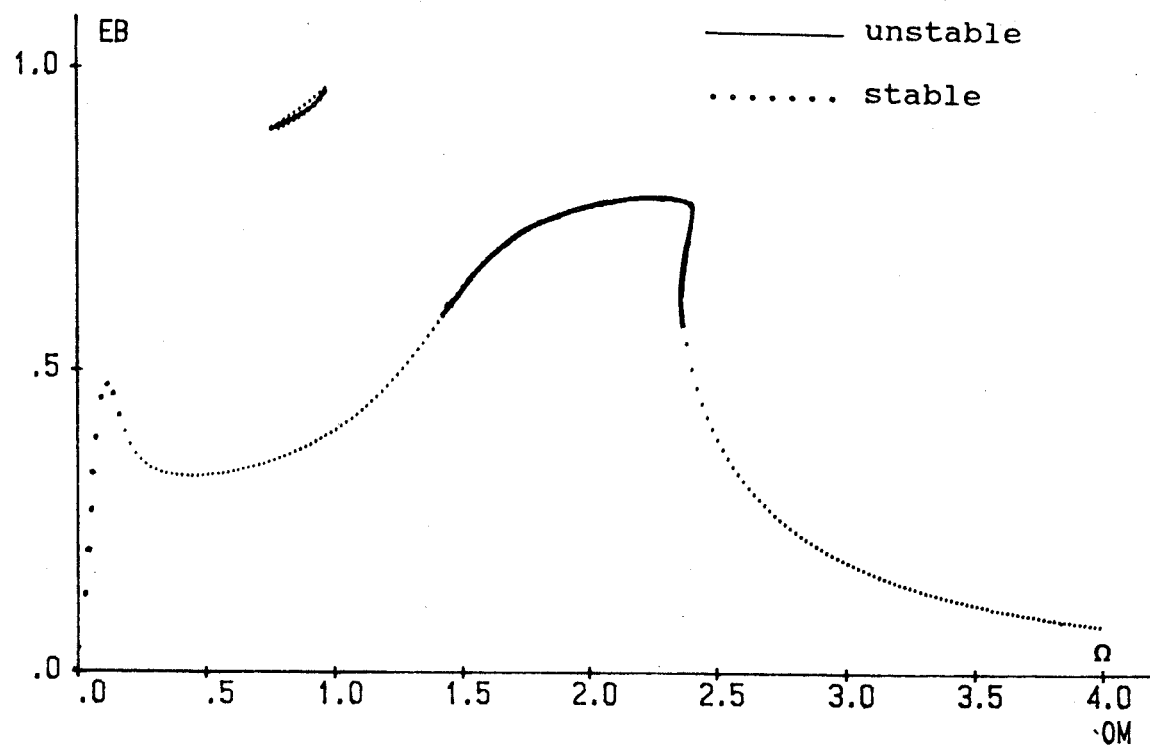


Fig.3 Stability analysis of system's circular response  
 $(U=0.4, \beta=0.005, \alpha=0.2, B=0.05, K=0.01)$

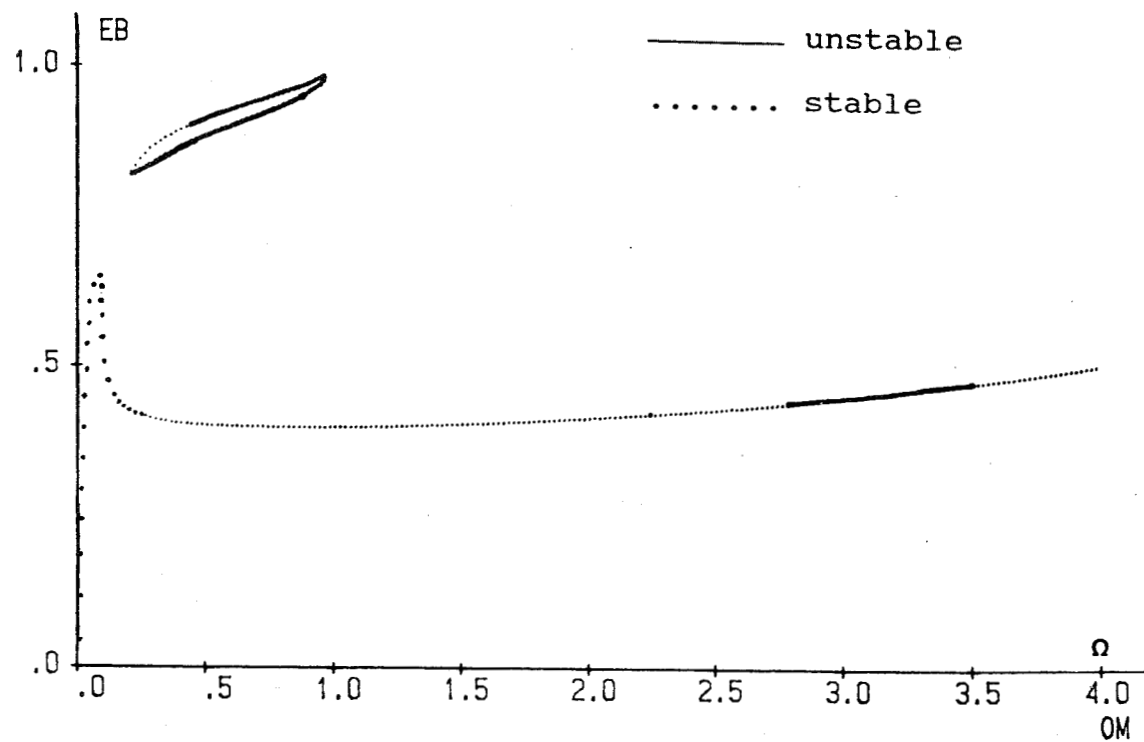


Fig.4 Stability of isolated bistable response  
( $U=0.4$ ,  $\beta=0.0005$ ,  $\alpha=0.01$ ,  $B=0.3$ ,  $K=0.001$ )

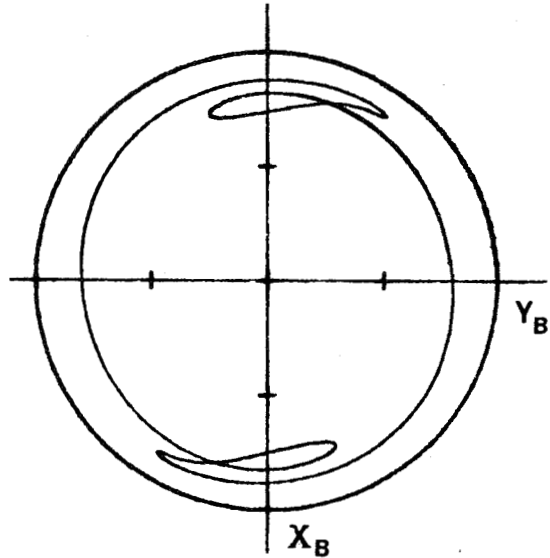


Fig.5 Nonsynchronous response in unstable region ( $U=0.4$ ,  $\beta=0.005$ ,  $\alpha=0.2$ ,  $B=0.05$ ,  $K=0.01$ ,  $\Omega=2.0$ )

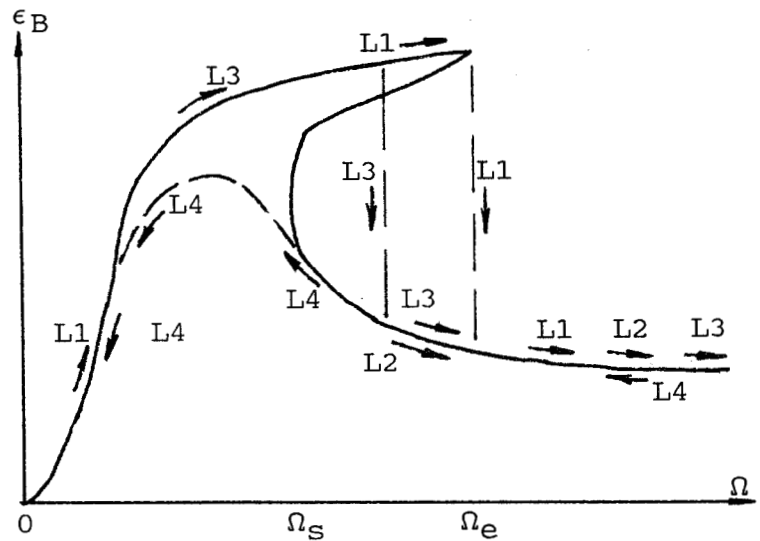


Fig.6 Schematic diagram of the influence of initial rotating speed on bistable jumping

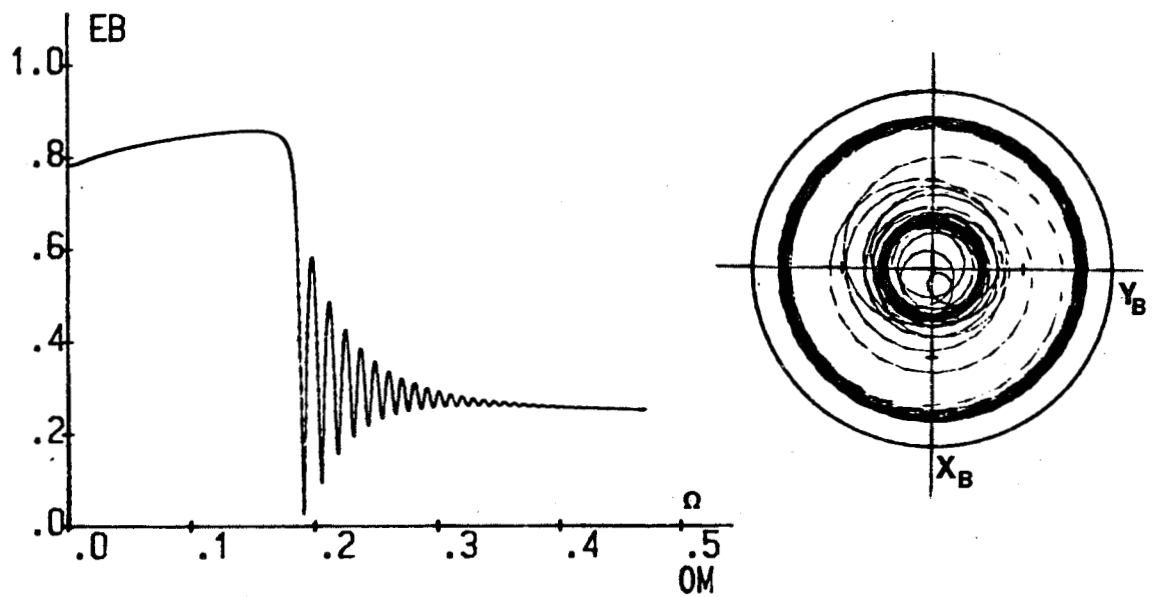


Fig.7 Bistable jumping response of accelerating through bistable region ( $U=0.25$ ,  $\beta=0.0005$ ,  $\alpha=0.1$ ,  $B=0.05$ ,  $K=0.2$ ,  $\Omega_0=0.42$ ,  $\Gamma=0.0005$ )

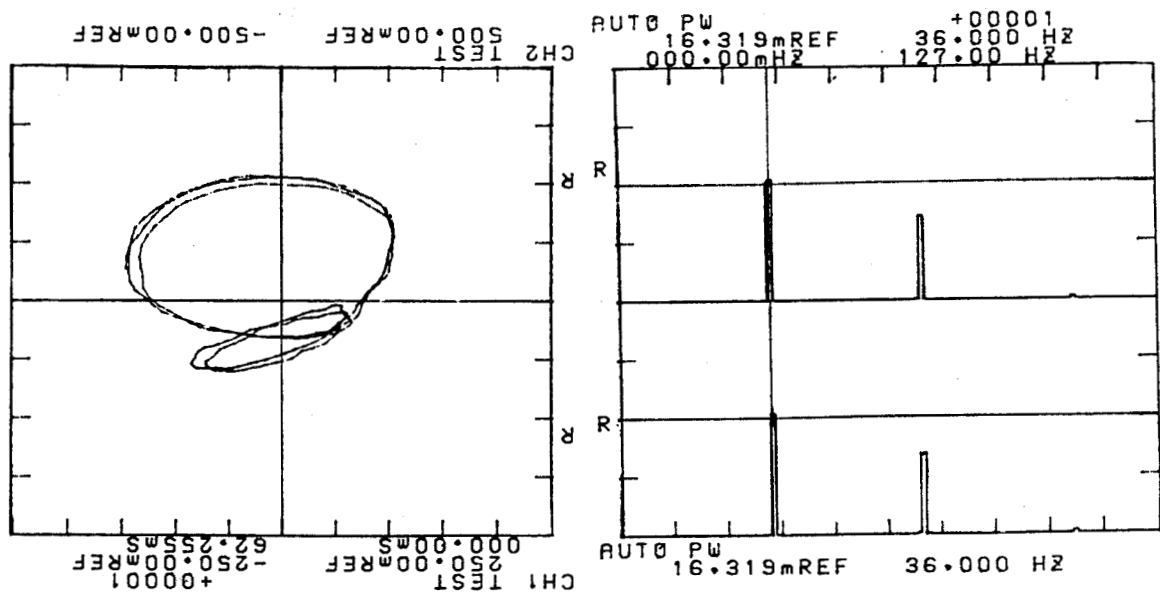


Fig.8 System's 1/2 subharmonic response by experiment ( $L=1.2$  cm,  $C/R=0.5\%$ ,  $m_u=10.5$  g,  $n=4320$  rpm)

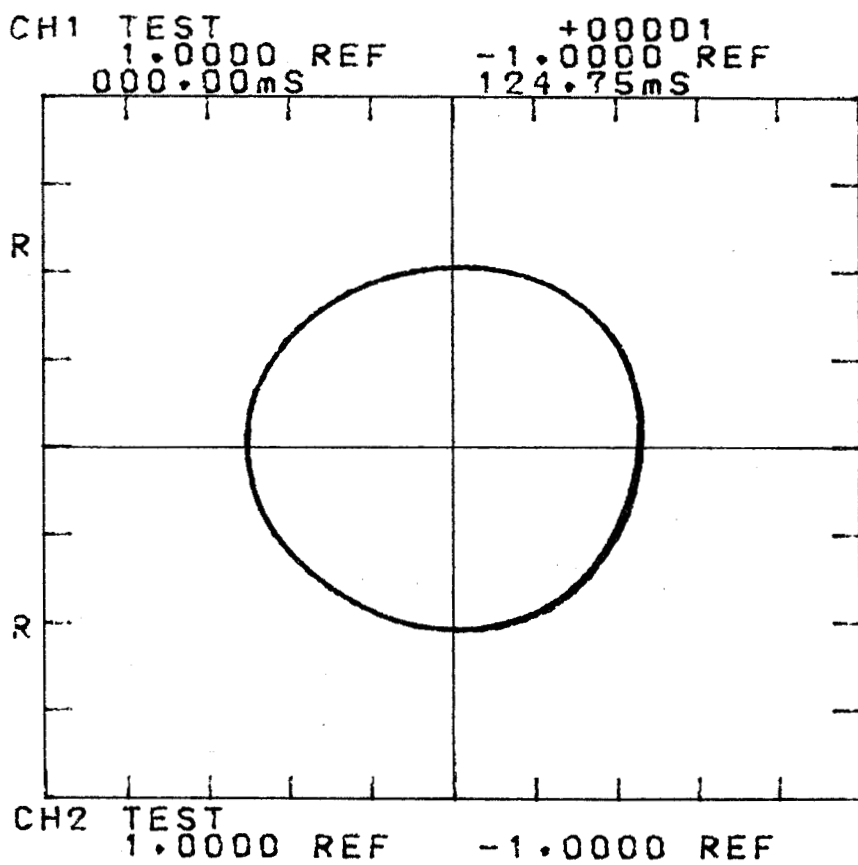


Fig.9 System's synchronous response by experiment  
( $L=1.6\text{cm}$ ,  $C/R=0.1\%$ ,  $m_u=7.6\text{g}$ ,  $n=5280\text{rpm}$ )

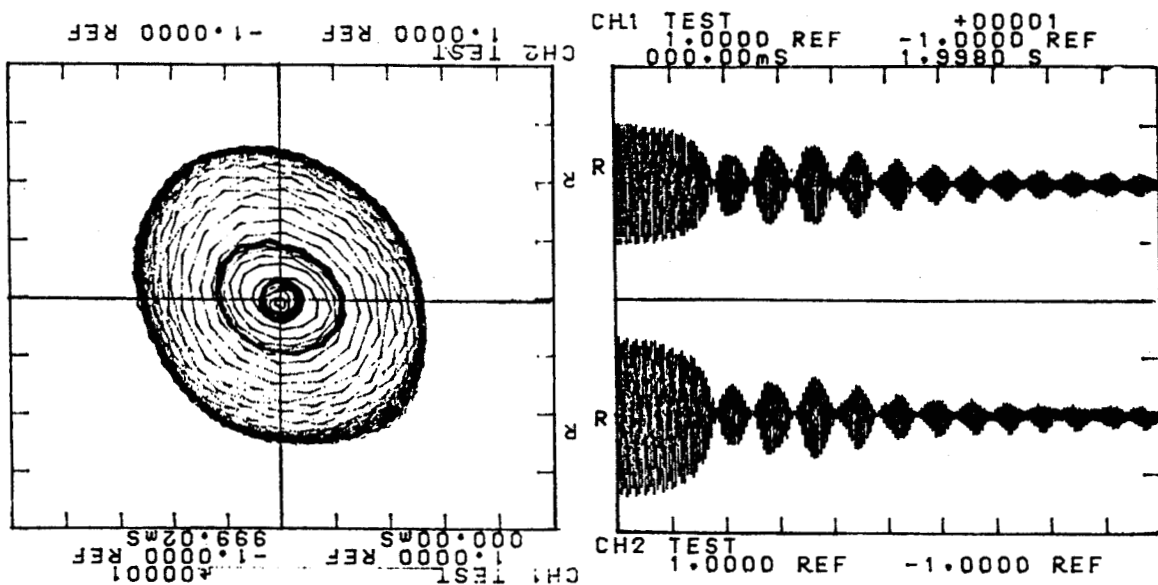


Fig.10 System's bistable response by experiment  
( $L=1.2\text{cm}$ ,  $C/R=0.1\%$ ,  $m_u=4.6\text{g}$ ,  $n=5430\text{rpm}$ )